The first gamma-ray outburst of a narrow-line Seyfert 1 galaxy: the case of PMN J0948+0022 in 2010 July

L. Foschini,[1]★ G. Ghisellini,[1] Y. Y. Kovalev,[2,3] M. L. Lister,[4] F. D'Ammando,[5]†
D. J. Thompson,[6]† A. Tramacere,[7]† E. Angelakis,[3] D. Donato,[8,9]† A. Falcone,[10]
L. Fuhrmann,[3]† M. Hauser,[11] Yu. A. Kovalev,[2] K. Mannheim,[12] L. Maraschi,[1]
W. Max-Moerbeck,[13]† I. Nestoras,[3]† V. Pavlidou,[13]† T. J. Pearson,[13]†
A. B. Pushkarev,[3,14,15] A. C. S. Readhead,[13]† J. L. Richards,[13]† M. A. Stevenson,[13]†
G. Tagliaferri,[1] O. Tibolla,[12]† F. Tavecchio[1] and S. Wagner[11]

[1]*INAF – Osservatorio Astronomico di Brera, via E. Bianchi 46, 23807 Merate (LC), Italy*
[2]*Astro Space Center of the Lebedev Physical Institute, Profsoyuznaya 84/32, 117997 Moscow, Russia*
[3]*Max-Planck-Institut für Radioastronomie, Auf dem Hügel 69, D-53121 Bonn, Germany*
[4]*Department of Physics, Purdue University, 525 Northwestern Avenue, West Lafayette, IN 47907, USA*
[5]*INAF – IASF-Palermo, Via Ugo La Malfa 153, 90146 Palermo, Italy*
[6]*NASA Goddard Space Flight Center, Greenbelt, MD 20771, USA*
[7]*ISDC Data Centre for Astrophysics, Chemin d'Ecogia 16, CH-1290 Versoix, Switzerland*
[8]*Center for Research and Exploration in Space Science and Technology and NASA Goddard Space Flight Center, Greenbelt, MD 20771, USA*
[9]*Department of Physics and Department of Astronomy, University of Maryland, College Park, MD 20742, USA*
[10]*Department of Astronomy and Astrophysics, Pennsylvania State University, University Park, PA 16802, USA*
[11]*Landessternwarte, Universität Heidelberg, Königstuhl, D-69117 Heidelberg, Germany*
[12]*Institut für Theoretische Physik und Astrophysik, University of Würzburg, 97074 Würzburg, Germany*
[13]*Cahill Center for Astronomy and Astrophysics, California Institute of Technology, Pasadena, CA 91125, USA*
[14]*Crimean Astrophysical Observatory, 98409 Nauchny, Crimea, Ukraine*
[15]*Pulkovo Observatory, 196140 St Petersburg, Russia*

ABSTRACT

We report on a multiwavelength campaign for the radio-loud narrow-line Seyfert 1 (NLS1) galaxy PMN J0948+0022 ($z = 0.5846$) performed in 2010 July–September and triggered by a high-energy γ-ray outburst observed by the Large Area Telescope onboard the *Fermi Gamma-ray Space Telescope*. The peak flux in the 0.1–100 GeV energy band exceeded, for the first time in this type of source, the value of $\sim 10^{-6}$ photon cm^{-2} s^{-1}, corresponding to an observed luminosity of $\sim 10^{48}$ erg s^{-1}. Although the source was too close to the Sun position to organize a densely sampled follow-up, it was possible to gather some multiwavelength data that confirmed the state of high activity across the sampled electromagnetic spectrum. The comparison of the spectral energy distribution of the NLS1 PMN J0948+0022 with that of a typical blazar – such as 3C 273 – shows that the power emitted at γ-rays is extreme.

Key words: galaxies: individual: PMN J0948+0022 – galaxies: jets – galaxies: Seyfert.

1 INTRODUCTION

Relativistic jets are the most extreme expression of the power that can be generated by supermassive black holes at the centres of galaxies. Their bolometric luminosity can reach values up to $\sim 10^{49-50}$ erg s^{-1}, peaking in the γ-ray (MeV–TeV) energy band. To date, two classes of active galactic nuclei (AGNs) are known to generate these structures: blazars and radio galaxies, both hosted in giant elliptical galaxies (Blandford & Rees 1978). The first class is composed of AGNs with the jet viewed at small angles, and therefore the effects of the special relativity play a dominant role in shaping the emission of the electromagnetic radiation. In the second class – radio galaxies – the jets are viewed at larger angles and therefore the Doppler boosting is less intense.

The recent discovery of variable γ-ray emission from four narrow-line Seyfert 1 (NLS1s) confirmed the presence of a third class of AGNs with relativistic jets (Abdo et al. 2009a,b,c; Foschini et al. 2010a), which was already suggested by the

---

★E-mail: luigi.foschini@brera.inaf.it
†Fermi LAT Member/Affiliated.

detection of variable radio emission with a flat or inverted spectrum (e.g. Grupe et al. 2000; Doi et al. 2006; Komossa et al. 2006; Yuan et al. 2008). This finding poses intriguing questions about jet systems and how these structures are generated. One of these sources, PMN J0948+0022 ($z = 0.5846$), is classified as a typical NLS1, i.e. full width at half-maximum [FWHM(Hβ) < 2000 km s^{-1}], [O III]/Hβ < 3, with the presence of the Fe II bump [see Pogge (2000) for a review on the characteristics of NLS1s]. However, it also displays strong, compact and variable radio emission, with an inverted spectrum, suggesting the presence of a relativistic jet (Zhou et al. 2003). The confirmation came with the detection of high-energy variable γ-rays by *Fermi*/Large Area Telescope (LAT; Abdo et al. 2009b, hereafter 'Discovery 2008'; Foschini et al. 2010a). A multiwavelength (MW) campaign performed in 2009 March–July displayed coordinated variability at all frequencies, thus confirming that the source detected by *Fermi*/LAT is indeed the high-energy counterpart of PMN J0948+0022 (Abdo et al. 2009c, hereafter 'MW Campaign 2009'). However, the variability observed in 2009 was much smaller in amplitude (more than a factor of 2 at γ-rays) with respect to the 2010 campaign.

The main differences between NLS1s and the other AGNs with jets are the optical spectrum and the radio morphology, which is quite compact and without extended structures (Doi et al. 2006; Komossa et al. 2006; Abdo et al. 2009c; Foschini et al. 2010a; Gu & Chen 2010). In addition, NLS1s are generally hosted in spiral galaxies (Deo, Crenshaw & Kraemer 2006; Zhou et al. 2006), which is at odds with the current observational paradigm linking very powerful jets with ellipticals (cf. e.g. Marscher 2010; see also Böttcher & Dermer 2002). Obviously, to make a proper comparison we would need either a direct imaging of the host galaxies of the four γ-NLS1s or the morphologies of a similar sample in terms of redshift and magnitude distribution. Our sources have redshifts between 0.061 and 0.585, while the work by Deo et al. (2006) is dedicated to a sample with $z < 0.03$ and Zhou et al. (2006) studied the morphology of NLS1s with $z < 0.1$, so there is only a partial overlap. At least one of the four NLS1s detected at γ-rays is definitely hosted by a spiral galaxy (1H 0323+342; see Zhou et al. 2007; Antón, Browne & Marchã 2008), while for the others there are no high-resolution observations available. Therefore, some halo of doubt remains.

Despite these uncertainties – worth studying – there are other novelties introduced by the γ-ray detection of NLS1s. The spectral energy distributions (SEDs) of the four γ-NLS1s point to AGNs with masses of the central black hole being in the range of 10^{6-8} M$_\odot$ and high accretion rates (up to 90 per cent of the Eddington value). These values are common for NLS1s (e.g. Boller, Brandt & Fink 1996; Collin & Kawaguchi 2004; Grupe 2004) but not for blazars or radio galaxies.

Another piece of the puzzle is given by the search for the parent population. Indeed, if γ-NLS1s seem to be similar to blazars, i.e. with the relativistic jet viewed at small angles, there should be a parent population with the jet viewed at large angles (as in the case of blazars versus radio galaxies). The first source of this type – PKS 0558−504 ($z = 0.137$) – has been recently found by Gliozzi et al. (2010). Therefore, it seems that NLS1s could be a set of low-mass systems 'parallel' to blazars and radio galaxies.

A key unknown in this research field was the power released by jets of γ-NLS1s. During the early observations and the 2009 MW campaign the maximum measured luminosity of PMN J0948+0022, the most powerful of these NLS1s, was $\sim 10^{47}$ erg s^{-1} (0.1–100 GeV). On the other hand, it is known that blazars can reach greater luminosities (see e.g. Ghisellini et al.
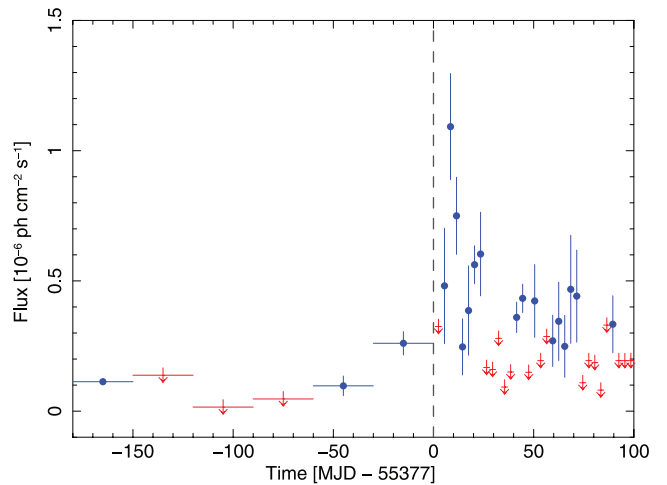

Figure 1. *Fermi*/LAT light curve (0.1–100 GeV) of PMN J0948+0022 in 2010, binned over 1 month during the first 6 months of 2010 and with a 3-d time bin for the period 2010 July–September. The value 0 on the abscissa corresponds to 2010 June 30 (MJD 55377). Blue points are detection with test statistic $TS > 10$ [equivalent to $\sim 3\sigma$; see Mattox et al. (1996) for the definition], while the others are 2σ upper limits. The abscissa has the same scale as Fig. 2, to make comparison easier.

2010), up to $\sim 10^{49}$ erg s^{-1} in the case of the brightest outbursts of 3C 454.3 (Foschini et al. 2010b; Bonnoli et al. 2011) or even in excess of 10^{50} erg s^{-1} in the recent episode of the gravitationally lensed quasar PKS 1830−21 (Ciprini et al. 2010). The question of the power could be studied in 2010 July, when PMN J0948+0022 underwent a period of intense activity (Donato et al. 2010; Foschini 2010) with a peak flux of $\sim 10^{-6}$ photon cm^{-2} s^{-1} (0.1–100 GeV), corresponding to an observed luminosity of $\sim 10^{48}$ erg s^{-1}. Here we report about the study of this period. Some very preliminary results have been presented in Foschini et al. (2010c).

In the following, we adopted a Λ cold dark matter cosmology as calculated in Komatsu et al. (2009) based on *Wilkinson Microwave Anisotropy Probe* results: $h = 0.71$, $\Omega_m = 0.27$, $\Omega_\Lambda = 0.73$ and with the Hubble–Lemaître constant $H_0 = 100\,h = 71$ km s^{-1} Mpc^{-1}.

2 DATA ANALYSIS

The analysis of the data from the different instruments and facilities participating in the present campaign was done in basically the same way as for that of 2009 (see the MW Campaign 2009 paper and references therein). There were some updates in the software used: *Swift*/X-Ray Telescope (XRT) and Ultraviolet Optical Telescope (UVOT) data were studied with the specific packages included in HEASOFT v. 6.10[1] and the calibration data base updated on 2010 September 30.

The light curve obtained from *Fermi*/LAT data is shown in Fig. 1, while Fig. 2 shows the optical (*R* filter) and radio (15-GHz) light curves from Automatic Telescope for Optical Monitoring for HESS (ATOM, Namibia) and Owens Valley Radio Observatory) (OVRO) 40-m telescope, the latter as part of an ongoing *Fermi* blazar monitoring programme (Richards et al. 2009). Multifrequency observations to measure spectral changes were also done at Effelsberg (Project F-GAMMA; Fuhrmann et al. 2007) and RATAN-600 (Kovalev et al. 1999), respectively. The study of the morphology
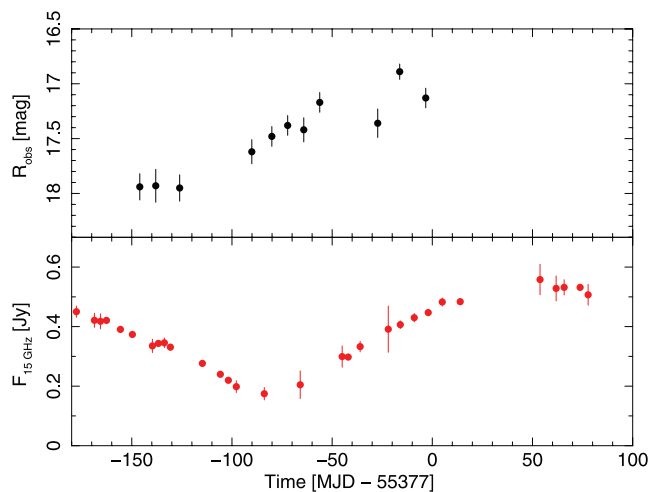

Figure 2. Light curve of PMN J0948+0022 at the optical (ATOM, *R* filter, top panel) and radio frequency (OVRO, 15 GHz, bottom panel). The abscissa has the same scale as Fig. 1, to make comparison easier. The value 0 corresponds to 2010 June 30 (MJD 55377).

Table 1. Summary of the spectral fitting of the *Fermi*/LAT data integrated on long time-scales. $F_{E > 100\,\text{MeV}}$ is in units of 10^{-6} photon cm^{-2} s^{-1}. The statistical measurement errors are at 1σ. Systematic errors are not included. The latest estimates for the adopted Instrument Response Function P6_V3_DIFFUSE are 10 per cent at 100 MeV, 5 per cent at 500 MeV and 20 per cent at 10 GeV, while the error in the photon index is ~0.1 (Rando et al. 2009).

Time period	$F_{E > 100\,\text{MeV}}$	Γ	*TS*
Jun 01–30	0.23 ± 0.01	2.77 ± 0.06	98
Jul 07–10	1.02 ± 0.02	2.55 ± 0.02	140
Aug 1–Sep 14	0.26 ± 0.01	2.74 ± 0.03	140

was done with Very Long Baseline Interferometry observations performed on 2010 September 17 as part of the Monitoring of Jets in Active Galactic Nuclei with VLBA Experiments (MOJAVE) monitoring programme[2] conducted with the Very Long Baseline Array (VLBA) at $\lambda = 2$ cm and provided high-resolution total intensity and linear polarization images. A detailed description of the MOJAVE programme as well as the method of observations, data processing and analysis is presented by Lister et al. (2009).

The source was close to the Sun in 2010 July, and therefore it was not possible to perform a densely sampled optical-to-X-ray follow-up. Only one X-ray observation close to the outburst remained and was performed by *Swift* on July 3 (ObsID 00038394002[3]), about 4 d before the outburst. A summary of XRT and UVOT analysis is displayed in Table 1, compared with the observations of 2008 December 5 (ObsID 00031306001, Discovery 2008) and of 2009 May 15 (ObsID 00031306006, the lowest X-ray flux measured during the MW Campaign 2009), when the source was in a low activity state at γ-rays.

The data available confirm the outburst first detected at γ-rays of the NLS1 PMN J0948+0022. The optical light curve from ATOM (*R* filter) indicates an increase in the optical activity with a change of about 1 mag during the early six months of 2010 (Fig. 2, top panel).

This trend is confirmed by the *Swift*/UVOT observation performed on July 3, when compared with an observation of the source at a low γ-ray state (2008 December 5 in the Discovery 2008; 2009 May 15 in the MW Campaign 2009): the decrease in the observed magnitude ranges from 0.6–0.7 mag in the v filter to 0.3–0.4 mag in the ultraviolet filters. The same behaviour was observed during the MW Campaign of 2009 March–July, when the source flux was decreasing, but showing stronger variability at optical frequencies rather than at the ultraviolet ones. This is likely to be due to the fact that ultraviolet frequencies sample the emission from the accretion disc, while the optical emission is mainly due to the synchrotron radiation.

The X-ray flux as measured by *Swift*/XRT was ~40 per cent greater than the value measured in the Discovery 2008 paper and a factor of ~2.4 greater with respect to the lowest flux measured during the MW Campaign 2009. The low statistics in the short observations of 2010 July 3 and 2009 May 15 prevent any conclusion on possible spectral changes.

At γ-rays, there was the most dramatic change in the emission of the electromagnetic radiation with an increase in flux by a factor of ~5 in the 0.1–100 GeV energy band. The outburst[4] (Fig. 1) was characterized by a first sharp increase in the flux on July 7 (Donato et al. 2010) with an e-folding time-scale[5] of 3.6 ± 1.8 d, reaching the peak value of ~10^{-6} photon cm^{-2} s^{-1} and remaining at such a level for about 4 d. On July 11 the source was not detected (with a 2σ upper limit of 2.7×10^{-7} photon cm^{-2} s^{-1}) and then it was detected again on July 12 above ~10^{-6} photon cm^{-2} s^{-1} (e−folding rise time of <1 d). After a few days of low activity, there was a second shorter outburst (Foschini 2010) with a flux of ~10^{-6} photon cm^{-2} s^{-1} and a rise time of <3 d. Then the source slowly returned to quiescence, with some occasional detection at moderate flux.

The spectral behaviour is more difficult to study. This comparative analysis should be considered with care, and the caveats about the comparison of fits over the whole energy band versus fits on separate energy bins are described in detail in section 4.4 of Abdo et al. (2010a). Nevertheless, the comparative analysis based on long time-scale (month) integration, thus with a more robust statistics than that available on short time-scales (Fig. 3, Table 1), indicates that there is some spectral hardening between the spectrum measured during the 4 d of the peak and the spectra measured on the data integrated on 2010 June and August–September. It is not possible to firmly establish if this is due to a change in the peak of the inverse-Compton emission, as occurred in the case of 3C 454.3 (see Bonnoli et al. 2011), or if it is due to an effective increase in the population of GeV photons.

The spectral evolution of the radio emission, as measured by Effelsberg and RATAN-600 (Fig. 4), instead indicates a progressive inversion of the spectral index between 4.8 and 10 GHz ($S_\nu \propto \nu^{-\alpha}$), changing from $\alpha = 0.02 \pm 0.03$ on 2010 May 1 (MJD 55317.83) to $\alpha = -0.81 \pm 0.02$ on 2010 June 26 (MJD 55373.77), an average $\alpha = -0.80 \pm 0.21$ measured in the period 2010 August 13–29, and up to a value of $\alpha = -1.0 \pm 0.1$ measured on 2010 September 18 (MJD 55457.45).

We compare these results with the MW Campaign of 2009 March–July, reported in Abdo et al. (2009c). In that case, the source

[4] Some information was derived from the analysis of the LAT light curve with 1-d time bin not shown here.
[5] That is the characteristic time τ to have an exponential increase or decrease in flux: $F(t) = F(t_0)\exp\left[-(t - t_0)/\tau\right]$.
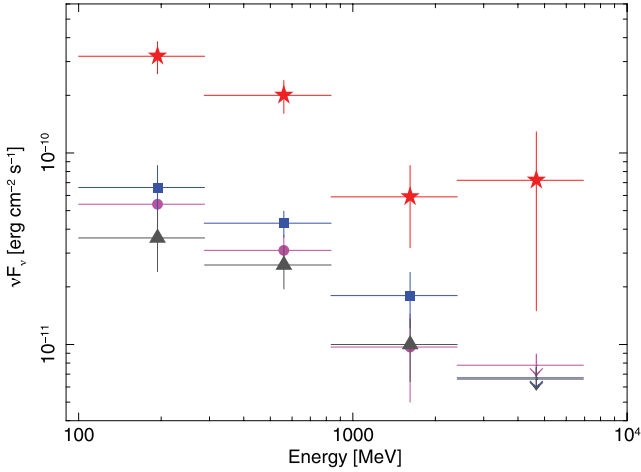
Figure 3. High-energy γ-ray SED of PMN J0948+0022. The red star symbols refer to the period of maximum flux (2010 July 7–10, 4 d), the blue squares indicate the emission integrated over the period 2010 August 1–September 15 (45 d), while the magenta circles are for the period 2010 June 1–30 (30 d). The grey triangles refer to the quiescence period of 1 month centred on 2008 December 5 (corresponding to the *Swift* observation; Abdo et al. 2009b). All the detections have $TS > 10$ ($\sim 3\sigma$; see Mattox et al. 1996). Upper limits are at the 2σ level. See also Table 1.
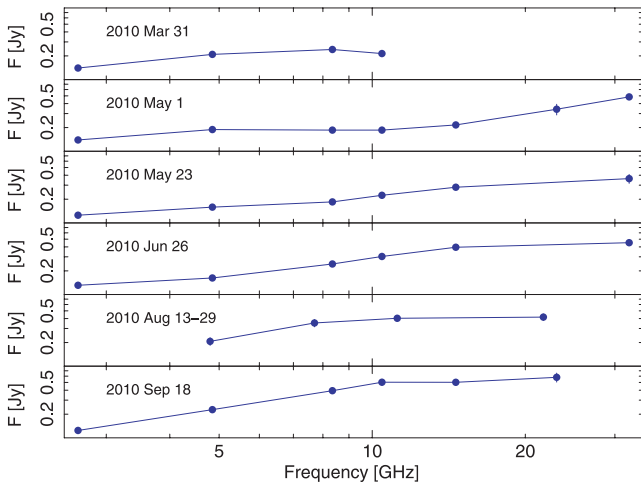
Figure 4. Spectral evolution at radio frequencies as measured by RATAN-600 (2010 August 13–29) and Effelsberg (all the remaining measurements).

was at a moderate high flux in 2009 April, peaking on April 1[6] with a flux of $(4.2 \pm 0.9) \times 10^{-7}$ photon cm^{-2} s^{-1} in the 0.1–100 GeV energy band and $\Gamma = 2.1 \pm 0.1$ [test statistic (TS) = 46; reanalysed in this work]. However, the flux integrated over the whole month of April gave a softer spectrum ($\Gamma = 2.7 \pm 0.2$; cf. Abdo et al. 2009c). In the 2010 July outburst, the γ-ray spectrum seemed softer before (June) and after (August–September) the burst, with some hardening during the peak of the emission (July). The 2010 July burst was a factor of ~ 2 greater than the 2009 April flare and also longer (more than 4 d versus 1 d).

It is also interesting to note the evolution of the radio emission, polarization and morphology as shown by the VLBA observations at 15 GHz (Fig. 5). The observation performed on 2010 September 17
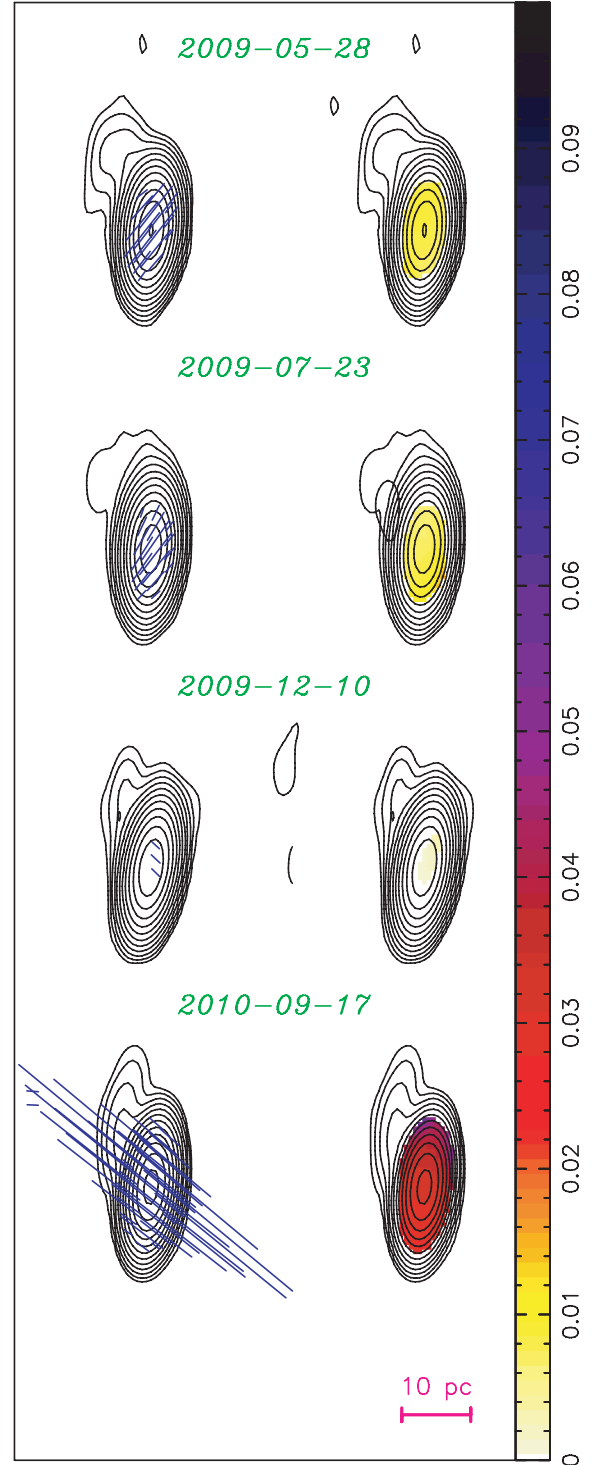
[6] As indicated in report 44 (2009 April 1–7) of the *Fermi Gamma Ray Sky* blog http://fermisky.blogspot.com/

Figure 5. Total intensity and linear polarization images observed by VLBA at 15 GHz in different epochs as part of the MOJAVE programme. Naturally weighted total intensity images are shown by black contours; the contours are in successive powers of two times the base contour level of 0.2 mJy beam^{-1}. The direction of electric polarization vectors is indicated on the left-hand side by blue sticks; their length is proportional to the polarized intensity. Linear fractional polarization is shown on the right-hand side overlaid according to the colour wedge.
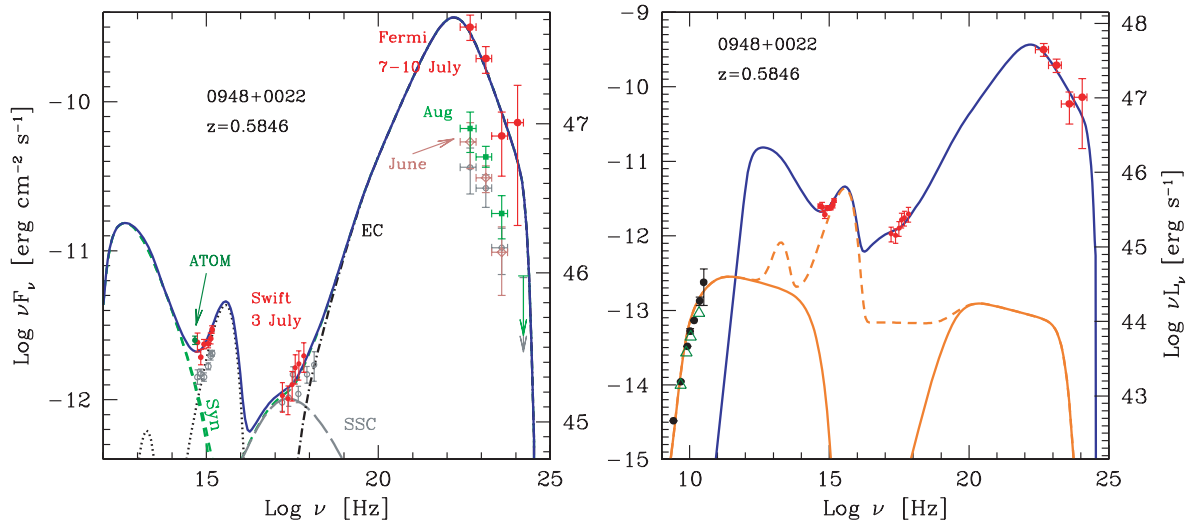
Figure 6. (Left-hand panel) SED of PMN J0948+0022. The grey symbols refer to the low activity period observed by *Swift* (2008 December 5) and *Fermi* (1 month centred on the *Swift* observation). The red symbols, used to model the SED, refer to July 7–10 (*Fermi*/LAT), July 3 (*Swift* XRT and UVOT) and June 26 (ATOM *R* filter). The model components are synchrotron (green dashed line), accretion disc and torus (black dotted line), synchrotron self-Compton (grey long-dashed line), external Compton (black dot–dashed line) and the sum of all of them (blue continuous line). (Right-hand panel) SED with radio data from RATAN-600 (August 13–29, green open triangles) and Effelsberg (September 18, black filled circles). The orange continuous lines are the result of the modelling of radio data (synchrotron plus external Compton with seed photons from the molecular torus). The dashed orange line is the emission from the torus and the accretion disc. The blue continuous line and the red points are the SED of the peak (July 7–10) shown in the left-hand panel.

shows a bright unresolved core with total parsec-scale flux density as high as 538 mJy and a high degree of polarization (3.3 per cent), greater than the values measured in 2009 (<1 per cent). Specifically, when studying the evolution from 2009 May (MW Campaign 2009) to 2010 September, we noted a drop in the polarized flux density in the third epoch, coupled with a swing of the electric vector polarization angle (EVPA) of about 90°, which is maintained in the last epoch, even with a much greater polarized flux density (a factor of ~6). A similar behaviour has been observed, for example, before the 2008 August outburst at γ-rays of the flat-spectrum radio quasar PKS 1502+106 ($z = 1.839$; Abdo et al. 2010b).

It is not possible to estimate the speed of the radio jet on the basis of these four epochs only, particularly as in the present case when the source is strikingly compact. Observations are continuing, and we anticipate having a robust speed estimate in the near future using a larger sample of epochs.

3 MODELLING OF THE SED

The SED shown in Fig. 6 (left-hand panel) has been fitted with the model described in Ghisellini & Tavecchio (2009), the same used in the previous works (Abdo et al. 2009a,b,c). The electromagnetic emission from a relativistic jet is modelled with different components: the synchrotron radiation plus the inverse-Compton emission derived by the interaction of the relativistic electrons with different types of seed photons (synchrotron, molecular torus, broad-line region, accretion disc, corona). We present here our favoured interpretation of the collected data. Changes in the model parameters are negligible with respect to variations of ±30 per cent in the 0.1–100 GeV flux or ±0.1 in the photon index (see section 4 of the Discovery 2008 paper for a more extended discussion on the impact of measurement errors on the calculations of the model parameters).

The γ-ray flux is most important, because it flags the jet power. The extreme Compton dominance suggests a Doppler factor greater than that measured during the MW Campaign 2009: therefore, we adopted in the model a bulk Lorentz factor $\Gamma = 16$ (versus 10 of

the MW Campaign 2009), with a jet viewing angle of 3° (versus 6°). This is one 'economical' possibility, in terms of energetic. It would be possible to obtain the same Compton dominance with a lower magnetic field, but with greater injected power (see below). In addition, it is worth noting that the magnetic field is linked to the X-ray emission through the synchrotron self-Compton process (it is peaking at these energies) and the only available X-ray measurement has been performed well before the beginning of the outburst (Table 2).

The energy distribution of the injected electrons (with a power of 2.1×10^{43} erg s^{-1} in the comoving frame) spans from $\gamma_{e,min} = 1$ to $\gamma_{e,max} = 2700$ and is described by a broken power-law model with indices γ_e^2 and $\gamma_e^{-3.2}$ below and above the break $\gamma_{e,break} = 200$, respectively, where γ_e indicates the random Lorentz factor of the electrons. The external Compton peak is produced by electrons with $\gamma_{e,peak} \simeq 170$, scattering off seed photons of the broad-line region.

Our model shows that most of the dissipation occurs at about 1.2×10^{17} cm (2600 Schwarzschild radii, within the broad-line region); the magnetic field is $B = 2$ G. The mass of the central black hole was fixed to the value of 1.5×10^8 M$_\odot$, as measured by fitting of the accretion disc emission (see Discovery 2008) and in agreement with the measurement by Zhou et al. (2003) by using FWHM of emission lines. The accretion rate is at 50 per cent of the Eddington value. The calculated jet powers (the output of the model) are $P_{radiative} = 5 \times 10^{45}$, $P_{magnetic} = 1.2 \times 10^{45}$, $P_{electrons} = 6 \times 10^{44}$ and $P_{protons} = 10^{47}$ erg s^{-1}, by assuming one proton per electron.

These values have to be compared with those reported in previous studies (specifically, see table 4 of the MW Campaign 2009 paper). The present values of the jet powers are generally greater, up to one order of magnitude in the case of the protons. Other differences with respect to the previous works are a lower magnetic field with respect to the average of the MW Campaign 2009 ($B = 4.1$ G), but similar to the value in Discovery 2008 ($B = 2.4$ G). The injected power is similar to the previous studies, but the shape is different, with a greater $\gamma_{e,max}$ (2700 versus 2000 and 1600, in the MW Campaign

Table 2. Summary of results from the analysis of the *Swift* data obtained on 2010 July 3 (ObsID 00038394002) compared with the observations of 2008 December 5 (ObsID 00031306001, Discovery 2008) and 2009 May 15 (ObsID 00031306006, MW Campaign 2009), both reanalysed here with the latest software (with consistent results), when the source was at a low γ-ray flux. The value of $N_{\rm H}$ was fixed to the Galactic column as measured by Kalberla et al. (2005).

			XRT (0.3–10 keV)			
ObsID	Date (YYYY/MM/DD)	Exp. (ks)	$N_{\rm H}$ ($10^{20}\,{\rm cm}^{-2}$)	Γ	Flux$_{0.3–10\,{\rm keV}}$ ($10^{-12}\,{\rm erg\,cm}^{-2}\,{\rm s}^{-1}$)	χ^2/d.o.f.
00038394002	2010/07/03	1.6	5.22	1.5 ± 0.3	5.5 ± 0.5	0.53/2
00038306006	2009/05/15	1.3	5.22	1.7 ± 0.3	2.3 ± 0.3	(*)
00031306001	2008/12/05	4.2	5.22	1.8 ± 0.2	3.9 ± 0.2	3.2/8

			UVOT (observed magnitudes)			
ObsID	v	b	u	$uvw1$	$uvm2$	$uvw2$
00038394002	17.6 ± 0.2	18.3 ± 0.1	17.24 ± 0.08	17.19 ± 0.07	17.34 ± 0.09	17.23 ± 0.06
00031306006	18.3 ± 0.2	18.4 ± 0.1	17.7 ± 0.1	17.43 ± 0.08	17.5 ± 0.1	17.65 ± 0.07
00031306001	18.2 ± 0.1	18.56 ± 0.08	17.79 ± 0.07	17.57 ± 0.06	17.63 ± 0.07	17.63 ± 0.05

*Low statistics. The fit has been performed by using the maximum likelihood (Cash 1979), obtaining a *c*-stat of 57 for 58 d.o.f.

2009 and Discovery 2008, respectively) and a smaller $\gamma_{\rm e,break}$ (200 versus 530 and 800, in the MW Campaign 2009 and Discovery 2008, respectively).

Since optical-to-X-ray data have been measured a few days before the outburst, it is possible that they are underestimated. If we assume an increase by a factor of 2–4 in the optical-to-X-ray fluxes, keeping the γ-ray flux to the observed peak value, then it is possible to model the SED with a relatively smaller bulk Lorentz factor ($\Gamma = 13$). The smaller beaming is compensated by an increase in the injected power of about one-third, plus a greater magnetic field ($B = 3.6\,{\rm G}$). The jet powers (protons, electrons, etc.) have negligible changes, because they are strongly dependent on the γ-ray flux.

The region emitting the optical-to-γ-ray flux is too compact to be responsible for the radio emission (its synchrotron flux is self-absorbed). This is confirmed by the variability analysis: the time-scales at γ-rays are short, of the order of days or even less than 1 d, thus requiring a very compact source. About 2 months after the outburst at γ-rays, the radio flux density reached its maximum (Fig. 2, bottom panel). During this period, the emitting region can move outwards and expand, thus becoming optically thin at radio frequencies. Moreover, near-simultaneous OVRO and MOJAVE observations indicate $\lesssim 50\,{\rm mJy}$ of arcsecond-scale flux density at 15 GHz; hence, nearly all of the radio emission in the source is generated on parsec scales. Therefore, to account for the radio emission, we considered an additional larger emitting zone (Fig. 6, right-hand panel). For the sake of simplicity, we assume the same bulk Lorentz factor of the optical-to-γ-rays fit ($\Gamma = 16$). This region is $\sim 0.6\,{\rm pc}$ in size, about two orders of magnitude larger than the γ-ray emitting region and farther (5.8 pc) from the central black hole. At this distance, the seed photons for the external Compton process are from the molecular torus, emitting at infrared wavelengths.

4 DISCUSSION AND CONCLUSION

We presented the results of an MW Campaign from radio to γ-rays performed in 2010 to study the evolution of the electromagnetic emission of the NLS1 galaxy PMN J0948+0022.

Despite all the caveats and uncertainties, what clearly emerges from this episode is the ability of an NLS1 to generate an extreme power ($\sim 10^{48}\,{\rm erg\,s}^{-1}$), when compared to that of a typical flat-spectrum radio quasar. Fig. 7 shows a comparison of the

SED (rest frame) of PMN J0948+0022 with that of the archetypical blazar 3C 273, known to have a strong disc emission too. At first look, the figure shows that the NLS1 has a more extreme Compton dominance: although its radio-to-X-ray luminosity is smaller than that of 3C 273, the γ-ray power is greater. If we renormalize the two SEDs by taking as a reference the peak due to the accretion disc emission, then it is necessary to multiply the values of PMN J0948+0022 by a factor of ~ 6, which in turn is roughly similar to the ratio of the masses of the central black holes ($1.5 \times 10^8\,{\rm M}_\odot$ for PMN J0948+0022 and $8 \times 10^8\,{\rm M}_\odot$ for 3C 273). By shifting upwards the SED of PMN J0948+0022 by this value, the differences in the radio-to-X-ray emission become negligible, while those at γ-rays are emphasized. At these energies, the differences can be explained with the different Doppler factor as a consequence of the different viewing angle (smaller in the case of this NLS1).
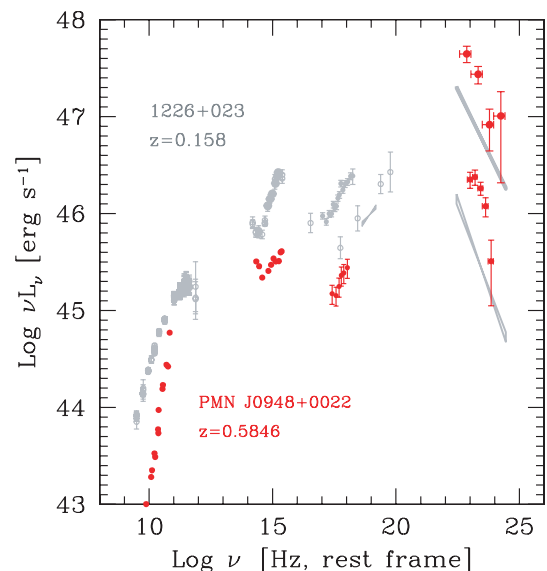

Figure 7. Comparison of the SEDs of the archetypical blazar 1226+023 (3C 273, grey symbols) and the NLS1 PMN J0948+0022 (red symbols). In the case of high-energy γ-rays, the minimum and maximum fluxes detected by *Fermi* are shown.

The basic findings of this work can be summarized as follows.

(i) The source reached an observed luminosity of $\sim10^{48}$ erg s^{-1} at γ-rays (0.1–100 GeV), with day-scale variability and some 'harder when brighter' spectral behaviour. This is the first time that such a power is measured from an NLS1. It confirms, beyond any reasonable doubt, that NLS1s can host relativistic jets as powerful as those in blazars and radio galaxies, despite the relatively low mass $(1.5 \times 10^8$ M$_\odot)$ and the rich environment due to a high accretion rate (50 per cent of the Eddington rate).

(ii) The coordinated variability observed at all the available frequencies confirms the typical behaviour of relativistic jets, as already shown during the MW Campaign 2009. Particularly, the radio emission peaked about 2 months after the outburst at γ-rays, although the radio spectral index was already inverted a couple of weeks before the peak in the GeV band. The optical flux changed about 1 mag (*R* filter) during the months before the outburst.

(iii) The morphology at 15 GHz still shows a very compact source (~10 pc size), despite the great power released at γ-rays. Comparison with previous observations in 2009 shows that the EVPA changed $\sim90°$ at some time between 2009 July and December, and this new value is maintained in 2010. The linear polarization fraction exceeds 3 per cent, a value greater than that measured in 2009 (<1 per cent).

(iv) The comparison with the SED of a typical blazar with a strong accretion disc (3C 273) shows that the Compton dominance is more extreme in the NLS1. The disagreement of the two SEDs can be accounted for by the differences in the masses of the central black hole and Doppler factor of the two jets.

REFERENCES

Abdo A. A. et al., 2009a, ApJ, 707, L142
Abdo A. A. et al., 2009b, ApJ, 699, 976 (Discovery 2008)
Abdo A. A. et al., 2009c, ApJ, 707, 727 (MW Campaign 2009)
Abdo A. A. et al., 2010a, ApJS, 188, 405
Abdo A. A. et al., 2010b, ApJ, 710, 810
Antón S., Browne I. W. A., Marchã M. J., 2008, A&A, 490, 583
Blandford R., Rees M., 1978, in Wolfe A. N., ed., Pittsburgh Conference on BL Lac Objects. Pittsburgh Univ. Press, Pittsburgh, PA, p. 328
Boller T., Brandt W. N., Fink H., 1996, A&A, 304, 53
Bonnoli G., Ghisellini G., Foschini L., Tavecchio F., Ghirlanda G., 2011, MNRAS, 410, 368
Böttcher M., Dermer C. D., 2002, ApJ, 564, 86
Cash W., 1979, ApJ, 228, 939
Ciprini S. et al., 2010, Astron. Telegram, 2943
Collin S., Kawaguchi T., 2004, A&A, 426, 797
Deo R. P., Crenshaw D. M., Kraemer S. B., 2006, AJ, 132, 321
Doi A., Nagai H., Asada K., Kameno S., Wajima K., Inoue M., 2006, PASJ, 58, 829
Donato D. et al., 2010, Astron. Telegram, 2733
Foschini L., 2010, Astron. Telegram, 2752
Foschini L. et al., 2010a, in Maraschi L., Ghisellini G., Della Ceca R., Tavecchio F., eds, ASP Conf. Ser. Vol. 427, Accretion and Ejection in AGN: A Global View. Astron. Soc. Pac., San Francisco, p. 243
Foschini L., Tagliaferri G., Ghisellini G., Ghirlanda G., Tavecchio F., Bonnoli G., 2010b, MNRAS, 408, 448
Foschini L. et al., 2010c, in Romero G., Sunyaev R., Belloni T., eds, Proc. IAU Symp. 275, Jets at All Scales. Cambridge Univ. Press, Cambridge, preprint (arXiv:1009.1055)
Fuhrmann L., Zensus J. A., Krichbaum T. P., Angelakis E., Readhead A. C. S., 2007, in Ritz S., Michelson P., Meegan C. A., eds, AIP Conf. Proc. 921, The First GLAST Symposium. Am. Inst. Phys., Melville, NY, p. 249
Ghisellini G., Tavecchio F., 2009, MNRAS, 397, 985
Ghisellini G., Tavecchio F., Foschini L., Ghirlanda G., Maraschi L., Celotti A., 2010, MNRAS, 402, 497
Gliozzi M., Papadakis I. E., Grupe D., Brinkmann W. P., Raeth C., Kedziora-Chudczer L., 2010, ApJ, 717, 1243
Grupe D., 2004, AJ, 127, 1799
Grupe D., Leighly K. M., Thomas H.-C., Laurent-Muehleisen S. A., 2000, A&A, 356, 11
Gu M., Chen Y., 2010, AJ, 139, 2612
Kalberla P. M. W., Burton W. B., Hartmann D., Arnal E. M., Bajaja E., Morras R., Pöppel W. G. L., 2005, A&A, 440, 775
Komatsu E. et al., 2009, ApJS, 180, 330
Komossa S., Voges W., Xu D., Mathur S., Adorf H.-M., Lemson G., Duschl W. J., Grupe D., 2006, AJ, 132, 531
Kovalev Y. Y., Nizhelsky N. A., Kovalev Yu. A., Berlin A. B., Zhekanis G. V., Mingaliev M. G., Bogdantsov A. V., 1999, A&AS, 139, 545
Lister M. L. et al., 2009, AJ, 137, 3718
Marscher A., 2010, in Belloni T., ed., Lecture Notes Phys. Vol. 794, The Jet Paradigm – From Microquasars to Quasars. Springer, Berlin, p. 173
Mattox J. R. et al., 1996, ApJ, 461, 396
Pogge R. W., 2000, New Astron. Rev., 44, 381
Rando R. et al., 2009, Proc. Int. Cosmic Rays Conf. Vol. 31, preprint (arXiv:0907.0626)
Richards J. L. et al., 2009, Proc. 2009 Fermi Symp., Washington, DC, preprint (arXiv:0912.3780)
Yuan W. M., Zhou H. Y., Komossa S., Dong X. B., Wang T. G., Lu H. L., Bai J. M., 2008, ApJ, 685, 801
Zhou H. Y., Wang T. G., Dong X. B., Zhou Y. Y., Li C., 2003, ApJ, 584, 147
Zhou H. Y., Wang T. G., Yuan W. M., Lu H. L., Dong X. B., Wang J. X., Lu Y. J., 2006, ApJS, 166, 128
Zhou H. Y. et al., 2007, ApJ, 658, L13

This paper has been typeset from a T$_{\rm E}$X/L$^{\rm A}$T$_{\rm E}$X file prepared by the author.